Stem Cell Reports
Article
OPEN ACCESS

A Cdx4-Sall4 Regulatory Module Controls the Transition from Mesoderm Formation to Embryonic Hematopoiesis

Elizabeth J. Paik,[1] Shaun Mahony,[2] Richard M. White,[3] Emily N. Price,[1] Anthony DiBiase,[1] Bilguujin Dorjsuren,[1] Christian Mosimann,[4] Alan J. Davidson,[5] David Gifford,[6] and Leonard I. Zon[1,*]
[1]Stem Cell Program and Division of Hematology/Oncology, Boston Children's Hospital, Harvard Stem Cell Institute, Harvard Medical School and Howard Hughes Medical Institute, Boston, MA 02115, USA
[2]Department of Biochemistry and Molecular Biology, Center for Eukaryotic Gene Regulation, Pennsylvania State University, University Park, PA 16802, USA
[3]Department of Cancer Biology and Genetics, Memorial Sloan-Kettering Cancer Center, New York, NY 10065, USA
[4]Institute of Molecular Life Sciences, University of Zurich, Winterthurerstrasse 190, 8057 Zurich, Switzerland
[5]Department of Molecular Medicine and Pathology, School of Medical Sciences, The University of Auckland, Auckland 1142, New Zealand
[6]Computer Science and Artificial Intelligence Laboratory, Massachusetts Institute of Technology, Cambridge, MA 02139, USA
*Correspondence: zon@enders.tch.harvard.edu
http://dx.doi.org/10.1016/j.stemcr.2013.10.001

SUMMARY

Deletion of *caudal*/*cdx* genes alters *hox* gene expression and causes defects in posterior tissues and hematopoiesis. Yet, the defects in *hox* gene expression only partially explain these phenotypes. To gain deeper insight into Cdx4 function, we performed chromatin immunoprecipitation sequencing (ChIP-seq) combined with gene-expression profiling in zebrafish, and identified the transcription factor *spalt-like 4* (*sall4*) as a Cdx4 target. ChIP-seq revealed that Sall4 bound to its own gene locus and the *cdx4* locus. Expression profiling showed that Cdx4 and Sall4 coregulate genes that initiate hematopoiesis, such as *hox*, *scl*, and *lmo2*. Combined *cdx4*/*sall4* gene knockdown impaired erythropoiesis, and overexpression of the Cdx4 and Sall4 target genes *scl* and *lmo2* together rescued the erythroid program. These findings suggest that auto- and cross-regulation of Cdx4 and Sall4 establish a stable molecular circuit in the mesoderm that facilitates the activation of the blood-specific program as development proceeds.

INTRODUCTION

Primitive hematopoietic progenitors arise from the yolk sac in mammals and generate red blood cells (RBCs), thereby providing oxygen to the rapidly developing embryos (Orkin and Zon, 2008). In zebrafish, equivalent cells arise from the lateral plate mesoderm (LPM), where anteriorly located cells give rise to myeloid cells and posteriorly located cells produce mostly RBCs. The first hematopoietic progenitors appear bilaterally from the 2- to 3-somite stage and express the transcription factor (TF) genes *fli1a*, *scl*, and *lmo2* (Liao et al., 1998; Thompson et al., 1998). By the 5-somite stage, posterior LPM cells are specified to the RBC lineage expressing *gata1* (Davidson et al., 2003; Detrich et al., 1995). As embryos develop, these bilateral stripes merge, creating the intermediate cell mass (ICM) region (Detrich et al., 1995). By 24 hr postfertilization (hpf), the embryonic RBCs start circulating.

Cdx4, a member of the caudal family, has been linked to embryonic hematopoiesis and leukemogenesis (Bansal et al., 2006; Davidson et al., 2003; Wang et al., 2005). The *Cdx* genes encode homeodomain-containing TFs that are known as master regulators of the *Hox* genes, and help establish the anterior-posterior (A-P) axis (Pownall et al., 1996; Subramanian et al., 1995). Mammals have three paralogs of the *Cdx* family (*Cdx1*, *Cdx2*, and *Cdx4*) that are expressed in the posterior tissues of the embryo (Young and Deschamps, 2009). Targeted knockout of *Cdx* genes demonstrated their roles in paraxial mesoderm, neurectoderm, and endoderm formation in mice (Chawengsaksophak et al., 2004; Gao et al., 2009; van den Akker et al., 2002; van Nes et al., 2006; Young et al., 2009). For example, *Cdx2/4* compound knockout mice show a truncated axial skeleton, decreased presomitic mesoderm, and defective caudal hindgut endoderm and placenta, indicating that *Cdx* genes function redundantly in mesendodermal tissue formation (van Nes et al., 2006; Young et al., 2009). Zebrafish also have three *cdx* paralogs: *cdx1a*, *cdx1b*, and *cdx4*. $cdx4^{-/-}$ embryos display shortened tail and neurectoderm defects, which are enhanced when *cdx1a* is also knocked down (Davidson et al., 2003; Davidson and Zon, 2006; Shimizu et al., 2006).

Zebrafish $cdx4^{-/-}$ embryos display a severe anemia, with decreased levels of *scl*, *lmo2*, and *gata1* expression in the posterior LPM (Davidson et al., 2003). This function of Cdx4 in hematopoiesis is conserved in murine embryonic stem cells (ESCs), where *Cdx4* overexpression increases erythroid, megakaryocyte, granulocyte, and macrophage lineage formation (Wang et al., 2005). Compound *Cdx* knockout in murine ESCs also leads to failures in hematopoietic differentiation (Wang et al., 2008). In addition to embryonic hematopoiesis, *Cdx* members are implicated in leukemogenesis, as shown by *CDX2* translocations in acute myeloid leukemia (AML) patients, and leukemia

seen in mice with *Cdx4* overexpression in bone marrow (Bansal et al., 2006; Scholl et al., 2007).

Many of the functions of *Cdx* have been linked to its ability to regulate *Hox* gene transcription (Young and Deschamps, 2009). However, an impact on *Hox* gene regulation does not explain all the defects in *Cdx* mutants. For example, conditional *Cdx2* knockout mice show defects in endoderm and presomitic mesoderm formation independently of *Hox* genes (Gao et al., 2009; Savory et al., 2009a). In addition, overexpression of anterior *hox* genes does not rescue the hindbrain defects seen in $cdx4^{-/-}/cdx1a^{mo}$ zebrafish (Skromne et al., 2007). These results suggest that *Cdx* function cannot be explained solely by *Hox* genes, and there must be other critical downstream genes.

Advances in chromatin immunoprecipitation sequencing (ChIP-seq) technology have helped investigators decipher complex transcriptional networks in many biological systems in a global manner. In ESCs, ChIP-seq experiments revealed that Oct4, Nanog, Sox2, and Sall4 share *cis*-regulatory modules and regulate each other to maintain pluripotency (Lim et al., 2008; Loh et al., 2006). Similar global studies were conducted in developing *Drosophila* and zebrafish embryos (Morley et al., 2009; Sandmann et al., 2006, 2007). Here, we used a genome-wide approach to identify direct Cdx4 target genes in zebrafish embryos by implementing ChIP-seq and microarray expression profiling. We show that the zinc-finger TF gene *sall4* is a downstream target of Cdx4. ChIP-seq analysis of Sall4 similarly demonstrates that it binds to its own promoter and *cdx4* regulatory elements. Gene-expression studies demonstrate that Cdx4 and Sall4 directly activate *hox* genes and hematopoietic genes. Cdx4 and Sall4 genetically interact during ventral mesoderm development, consistent with a role for these TFs in the early expression of hematopoietic TFs. Together, these results suggest that auto- and cross-regulatory interactions between *cdx4* and *sall4*, as well as coactivation of common gene targets, establish a key regulatory module that directs the transition of the mesoderm into blood.

RESULTS

Identification of Direct Cdx4 Downstream Target Genes

To identify direct Cdx4 downstream target genes, we conducted ChIP-seq using zebrafish embryos in the bud stage, the stage just prior to the emergence of *fli1a*+, *scl*+, and *lmo2*+ hematopoietic progenitors. Since ChIP-quality zebrafish Cdx4 antibodies were not available, a full-length, C-terminally myc-tagged zebrafish Cdx4 was overexpressed and myc antibodies were used for immunoprecipitation. This technique has been used successfully for Nanog ChIP-seq analysis in zebrafish (Xu et al., 2012). To reduce nonspecific Cdx4 binding, *cdx4-myc* mRNA was injected at a dose that rescued $cdx4^{-/-}$ animals but did not cause morphological changes in $cdx4^{+/-}$ animals (Figure S1A available online).

Cdx4 ChIP-seq yielded 5,166 binding events, which corresponded to 1,343 proximal genes (distance to the transcriptional start site: ±10 kb). De novo motif analysis using the top 500 bound sequences gave an ATAAA motif, which was reported as the Cdx2 consensus DNA-binding motif (Figure 1A; Nishiyama et al., 2009; Verzi et al., 2010). The Cdx family members share a highly similar homeodomain and are functionally redundant (Savory et al., 2009b). The most well-known targets of the Cdx family members are *Hox* genes (Charité et al., 1998; Knittel et al., 1995; Subramanian et al., 1995), and strong Cdx4 binding was found across all seven clusters of *hox* genes in the zebrafish genome (Figures 1B and S1B). Cdx4 bound to its own locus, suggesting possible autoregulation (Figure 1C).

Binding to specific signaling pathways and gene programs does not necessarily mean that Cdx4 regulates their transcription at the time of the analysis. To demonstrate that Cdx4 binding to these loci leads to transcriptional changes during the LPM-to-hematopoietic transition, we evaluated gene expression by microarrays. Given the redundancy between Cdx4 and Cdx1a, we used 2-somite stage embryos coinjected with *cdx4* and *cdx1a* morpholinos ($cdx4^{mo}/cdx1a^{mo}$) because these embryos display the most severe loss-of-Cdx-function phenotype (Davidson and Zon, 2006). To systematically compare the ChIP-seq target list with the microarray data, we ranked differentially regulated genes in the $cdx4^{mo}/cdx1a^{mo}$ microarray data using the Gene Set Enrichment Analysis (GSEA) and compared them with Cdx4 binding (Subramanian et al., 2005). This analysis showed that the Cdx4-bound genes were highly downregulated in the $cdx4^{mo}/cdx1a^{mo}$ microarray (normalized enrichment score [NES] = 1.76, false discovery rate [FDR] = 0.1; Figure S1C), suggesting that Cdx4 works as a transcriptional activator, consistent with data previously reported with Cdx2 (Nishiyama et al., 2009; Verzi et al., 2011). For example, 26 of the 44 Cdx4-bound *hox* genes and the Cdx4 bound-Wnt pathway genes, including *axin1*, *axin2*, and *wnt5b*, were all downregulated, confirming the Cdx4 ChIP-seq data (Figure S1D). These results suggest that a subset of the Cdx4-binding sites detected by ChIP-seq is indeed transcriptionally regulated by Cdx4.

sall4 Is a Direct Downstream Target of Cdx4

spalt-like 4 (*sall4*) was strongly downregulated in $cdx4^{mo}/cdx1a^{mo}$ and bound by Cdx4 (Figures 1D and S1E). The *spalt* gene was first identified in *Drosophila*, where its mutation caused homeotic changes in the posterior head and

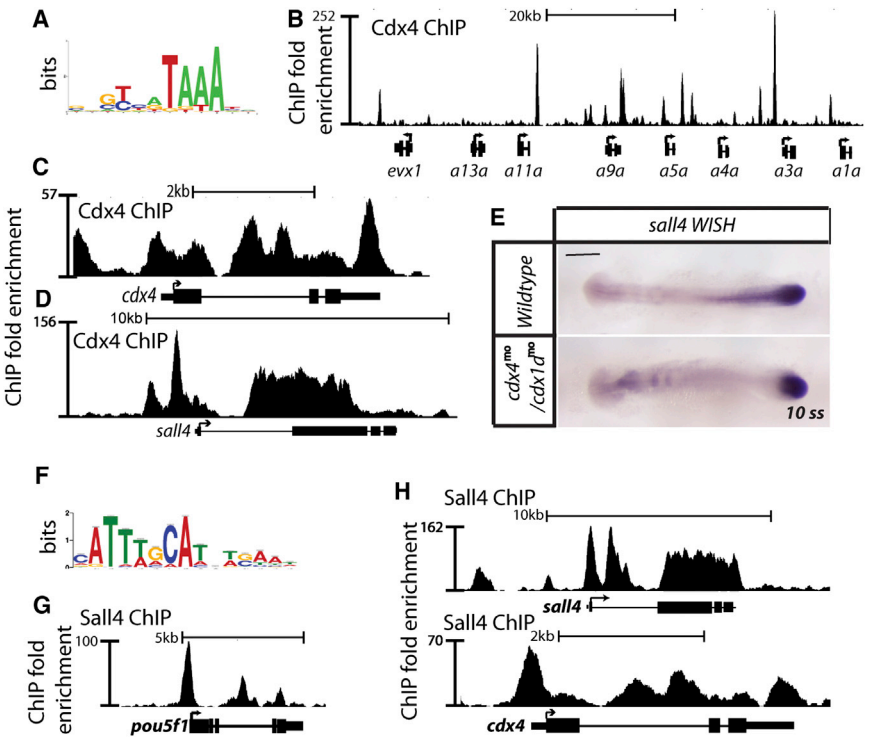

Figure 1. Cdx4 and Sall4 Bind to Each Other's Genomic Locus

(A) Cdx4-binding sites are enriched for the ATAAA motif. The most enriched motif was identified using MEME (Bailey and Elkan, 1994).

(B) Gene track of the *hox aa* locus, showing Cdx4 binding at genomic regions along the x axis and the total number of reads on the y axis.

(C) Gene track of the *cdx4* locus, showing Cdx4 binding to its own locus.

(D) Gene track of the *sall4* locus, showing Cdx4 binding to *sall4* locus.

(E) WISH of *sall4* mRNA expression level in 10-somite stage wild-type embryos and $cdx4^{mo}/cdx1a^{mo}$. Scale bar = 200 μm.

(F) Sall4-binding sites are enriched for the ATTTGCAT motif, an *Oct4* motif.

(G) Gene track of the *pou5f1* locus, showing Sall4 binding.

(H) Gene track of *sall4* and *cdx4* loci, showing Sall4 binding.

See also Figure S1.

anterior tail region (Frei et al., 1988; Jürgens, 1988). Its homologs are highly expressed in the developing tail tip region in both chickens and frogs (Barembaum and Bronner-Fraser, 2004; Neff et al., 2005). In addition, *SALL4* transgenic mice develop AML, reminiscent of mice that were transplanted with mCdx4-transduced bone marrow (Bansal et al., 2006; Ma et al., 2006). Because the *cdx* homolog, *caudal*, is involved in homeotic switches in *Drosophila* and is highly enriched in the posterior region, the *sall4* gene made an excellent candidate to act downstream of *cdx4*.

To validate the microarray data indicating that a loss of Cdx function leads to decreased *sall4* transcription, we conducted whole-mount in situ hybridization (WISH) was conducted in 10-somite stage $cdx4^{mo}/cdx1a^{mo}$ embryos. *sall4* expression was downregulated in these embryos, consistent with the Cdx factors directly regulating *sall4* transcription (Figure 1E). We also found that *cdx4* and *sall4* are spatially and temporally coexpressed (Figure S1F). Taken together, these results strongly suggest that Cdx4 regulates *sall4* transcription during zebrafish development.

Sall4 Binds to the *cdx4* Locus

To examine Sall4 downstream target genes, we conducted ChIP-seq on bud-stage zebrafish embryos injected with 100 pg of *sall4-myc* mRNA, which does not cause morphological defects (Figure S1G). Sall4 ChIP-seq resulted in 9,747 binding events that corresponded to 1,832 proximal genes. De novo motif analysis gave the ATTTGCAT motif, which is known as the *Oct4* motif (Figure 1F; Loh et al., 2006). In addition, Sall4-myc bound to the *oct4/pou5f1* locus, consistent with reports showing that Sall4 is a part of the core ESC complex with Oct4 (Figure 1G; Rao et al., 2010; van den Berg et al., 2010; Wu et al., 2006). Sall4 binds to its own locus, suggesting autoregulation, and to the *cdx4* locus, indicating cross-regulatory interactions between Sall4 and Cdx4 (Figures 1H and S1H).

Cdx4 and Sall4 Coregulate Genes Responsible for the Mesoderm-to-Blood Transition

The Sall4 ChIP-seq analysis showed a substantial overlap in binding sites with Cdx4 across the genome (Figure 2A). When we compared the Cdx4-Sall4 cobound sites with the bud-stage zebrafish histone ChIP-seq data, we found that 44% of these sites overlapped with H3K27ac-enriched domains, whereas only 1.4% overlapped with H3K4me3-enriched domains. This indicates that Cdx4 and Sall4 cobinding corresponds to active enhancers (Figure 2B; Rada-Iglesias et al., 2011). A Gene Ontology (GO) analysis of the Cdx4-Sall4 cobound gene list revealed that the cobound group is enriched with genes associated with pattern specification and embryonic morphogenesis (Figure 2C).

To determine whether Cdx4 and Sall4 cobinding leads to a cooperative transcriptional output, we obtained gene-expression data from $cdx4^{mo}$, $sall4^{mo}$, and $cdx4^{mo}/sall4^{mo}$

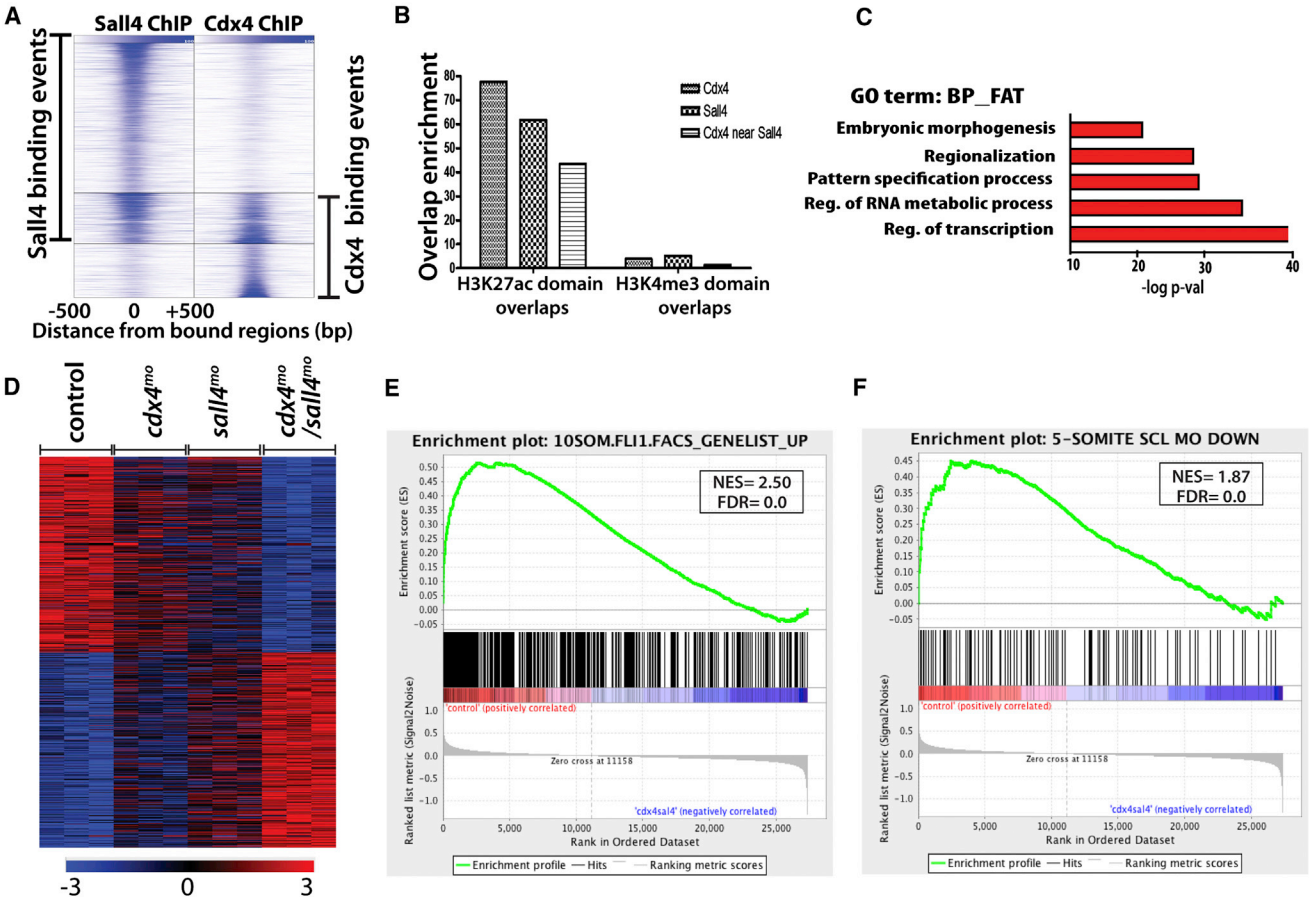

Figure 2. Cdx4 and Sall4 Coregulate Downstream Target Genes

(A) Genome-wide Cdx4 and Sall4 binding events. The two columns show enrichment over all Sall4 and Cdx4 binding sites, where the blue shading corresponds to the ChIP-seq read count in the region.

(B) Cdx4- and Sall4-bound regions are associated with H3K27ac histone marks. The bar graph shows the relative overlap of Cdx4-bound, Sall4-bound, and Cdx4-Sall4-cobound regions with H3K27ac (enhancer) and H3K4me3 (promoter) marks compared with background expectation. The overlap enrichment score calculates the percentage of bound sites that overlap (or are within 100 bp of) a chromatin mark domain and normalizes by the percentage of 10,000 random genomic sites that overlap (or are within 100 bp of) the same chromatin mark domains.

(C) GO Analysis of the Cdx4-Sall4 Cobound Genes

(D) Heatmap demonstrating the top 1,000 genes that show cooperation between the *cdx4* and *sall4* knockdown at the 10-somite stage. Genes that are only moderately affected in either single morphant show significantly greater effects in the 10-somite stage $cdx4^{mo}/sall4^{mo}$.

(E and F) GSEA-based comparison between $cdx4^{mo}/sall4^{mo}$ and known hematopoietic gene signatures.

(E) Comparison between *cdx4/sall4* and the GFP+ population from t10-somite stage Tg(*fli1a:GFP*) embryos.

(F) Comparison with genes downregulated in the 5-somite stage scl^{mo}. In both cases, the hematopoietic signature is strongly enriched in $cdx4^{mo}/sall4^{mo}$ compared with control embryos.

See also Figure S2.

embryos. To examine whether knockdown of both genes leads to a greater transcriptional change compared with single knockdowns, we compared the expression level in the double morphants with that in the single morphants (see Experimental Procedures for details). In both the 3- and 10-somite stage embryos, the double morphants exhibited enhanced down- or upregulation of mRNA expression compared with the single morphants (Figures 3D and S2A). At the 10-somite stage, the top ten most downregulated genes from double morphants included *hox* genes, indicating that in addition to being cobound to the *hox* gene loci, Cdx4 and Sall4 cooperate to regulate the *hox* gene transcriptional program (Figure S2B). In addition, these double morphants exhibit downregulation of non-hox gene members such as *gfi1.1* and *morc3b* (Figure S2B).

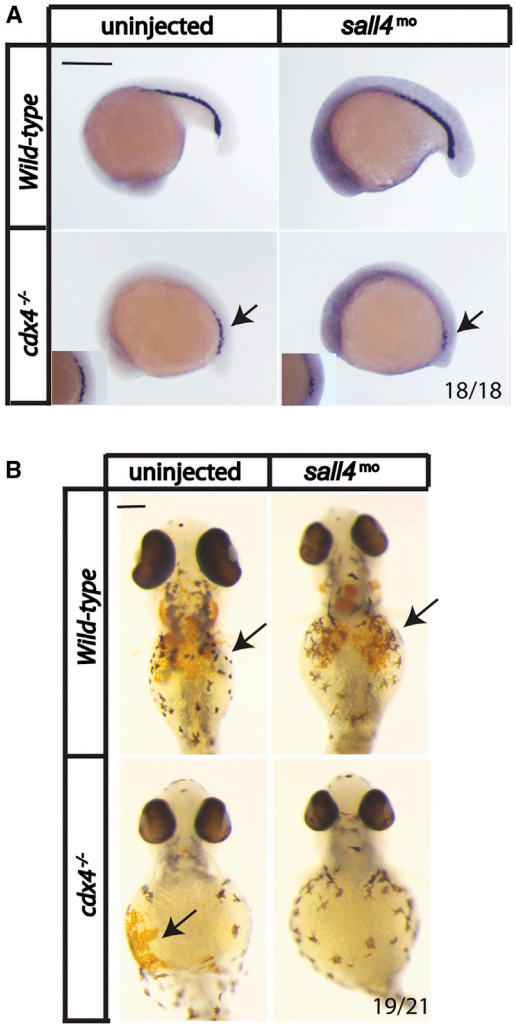

Figure 3. *sall4* Cooperates with *cdx4* in Zebrafish Hematopoiesis

(A) *gata1* WISH of 18-somite-stage wild-type or $cdx4^{-/-}$ embryos that were uninjected or $sall4^{mo}$ injected. *sall4* knockdown in the $cdx4^{-/-}$ background leads to a decrease in *gata1*+ cells (note the high-powered view).

(B) o-Dianisidine staining of 3 dpf wild-type or $cdx4^{-/-}$ embryos that were uninjected or $sall4^{mo}$ injected. $cdx4^{-/-}/sall4^{mo}$ embryos have fewer hemoglobinized RBCs. Arrows point to the stained RBCs in the embryos. Scale bar, 200 μm.

See also Figure S3.

We noted that a number of genes affected in the double morphants were those that are typically associated with primitive hematopoiesis (e.g., *gata1*, *gfi1.1*, and *znfl2*) (Detrich et al., 1995; Galloway et al., 2008; Wei et al., 2008). To globally address whether double morphants show defects in hematopoiesis, we used GSEA to compare the genes affected in $cdx4^{mo}/sall4^{mo}$ with the gene signatures of hematopoietic cells subjected to fluorescence-activated cell sorting (FACS) or morphants deficient in blood. The gene signature of the fli1a:GFP+ cells (the sorted population from the 10-somite stage Tg(*fli1a:GFP*) that express GFP in both blood and endothelial cells; Lawson and Weinstein, 2002) was highly enriched in the $cdx4^{mo}/sall4^{mo}$ gene-expression set (NES = 2.50, FDR = 0.0; Figure 3D). Genes that were downregulated in the scl^{mo} (which lacks a hemangioblast population; Dooley et al., 2005; Patterson et al., 2005) were also strongly enriched in the $cdx4^{mo}/sall4^{mo}$ (NES = 1.87, FDR = 0.0; Figure 3E). To determine whether the $cdx4^{mo}/sall4^{mo}$enrichment was specific to blood, was conducted additional GSEAs using endothelial (Wong et al., 2009), renal (O'Brien et al., 2011; Wingert and Davidson, 2011; Wingert et al., 2007), muscle (de la Serna et al., 2005), and neuron (Lein et al., 2007) gene sets (Figures S2C–S2F). Among these, only the endothelial gene set showed significant enrichment (NES = 2.47, FDR = 0.0; Figure S2C). This result is not surprising, because blood and endothelial populations share common TFs, especially during primitive hematopoiesis (Davidson and Zon, 2004). In contrast, the enrichment scores for other gene sets were not significant, indicating that $cdx4^{mo}/sall4^{mo}$ embryos show more specific defects in the hemangioblast population (Figures S2D–S2F). Taken together, the ChIP-seq and microarray data indicate that Cdx4 and Sall4 coregulate a set of genes involved in both embryonic pattern formation and primitive hematopoiesis.

sall4 and *cdx4* Functionally Interact during the Formation of RBCs

To demonstrate that *sall4* functionally interacts with *cdx4* during embryonic hematopoiesis, *sall4* was knocked down in $cdx4^{-/-}$ embryos. $cdx4^{+/-}$ zebrafish were crossed and $sall4^{mo}$ was injected into one-cell-stage embryos (Davidson et al., 2003; Harvey and Logan, 2006). Knockdown of *sall4* in either a $cdx4^{+/+}$ or $cdx4^{+/-}$ background resulted in a slight shortening of the A-P axis by 28 hpf, but had no effect on erythropoiesis.

Because $cdx4^{-/-}$ have fewer *gata1*+ cells in the ICM region and fewer RBCs later, we examined these phenotypes in *sall4* knockdowns in the background of $cdx4^{+/+}$, $cdx4^{+/-}$, and $cdx4^{-/-}$ embryos. At the 18-somite stage, the $cdx4/sall4^{mo}$ embryos had fewer *gata1*+ cells compared with the uninjected $cdx4^{-/-}$ embryos (Figure 3A). The $cdx4^{+/+}/sall4^{mo}$ or $cdx4^{+/-}/sall4^{mo}$ embryos did not show a decrease in *gata1*. Although the hematopoietic defect in the $cdx4^{-/-}/sall4^{mo}$ embryos was not as severe as that shown in the $cdx4^{mo}/cdx1a^{mo}$ embryos that completely lack *gata1* (Davidson and Zon, 2006), these studies indicate that Sall4 and Cdx4 functionally interact during erythroid progenitor formation (Figure 3A).

The injected embryos were grown to 3 days postfertilization (dpf), and o-dianisidine staining was conducted to

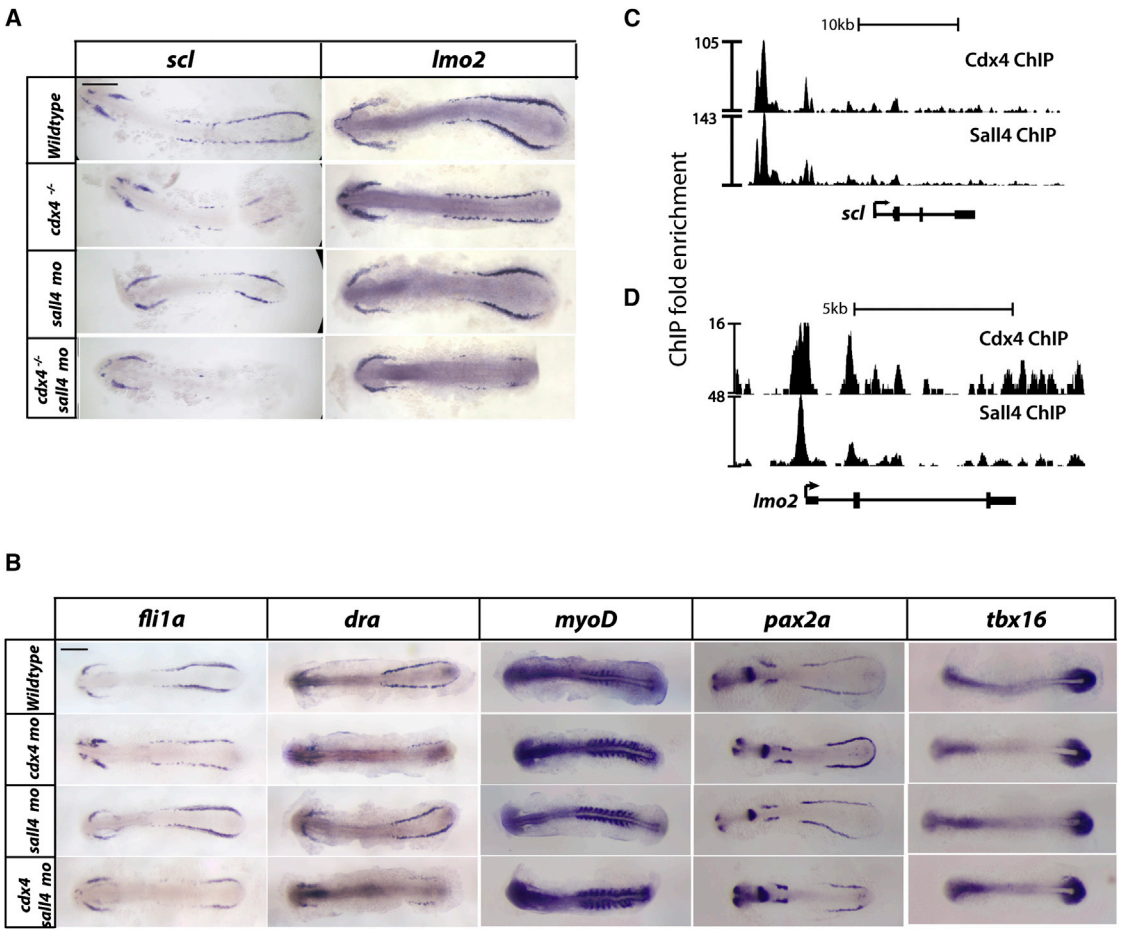

Figure 4. *scl* and *lmo2* Are Responsible for the Loss of RBCs Seen in *cdx4*$^{-/-}$;*sall4*^{mo} Embryos.
(A and B) *scl* (A) and *lmo2* (B) WISH at the 10-somite stage wild-type or *cdx4*$^{-/-}$ embryos that are either uninjected or *sall4*^{mo} injected. Embryos were flat-mounted, with the anterior end pointing to the left and the posterior end pointing to the right.
(C) *fli1a*, *draculin*, *pax2a*, *myoD*, and *tbx16* WISH in 10-somite stage wild-type, *cdx4*^{mo}, *sall4*^{mo}, *cdx4*^{mo}/*sall4*^{mo} embryos. All scale bars, 200 μm.
(D and E) Gene track of the *scl* (D) and *lmo2* (E) loci, showing Cdx4 and Sall4 binding.
See also Figure S4.

examine hemoglobinized RBCs (Ransom et al., 1996). As previously reported (Davidson et al., 2003), *cdx4*$^{-/-}$ embryos showed a decreased number of hemoglobinized RBCs compared with wild-type or *cdx4*$^{+/-}$ embryos. When *sall4*^{mo} was injected, these *cdx4*$^{-/-}$ embryos showed even fewer hemoglobinized RBCs, consistent with *sall4* cooperating with *cdx4* during erythropoiesis (Figure 3B, arrow). The posterior mesoderm was also critically affected in *cdx4*$^{-/-}$/*sall4*^{mo} embryos, as evidenced by the size of the tail (Figure S3).

Loss of *scl* and *lmo2* Is Responsible for the Lack of RBCs in *cdx4*$^{-/-}$/*sall4*^{mo} Embryos

The loss of RBCs seen in the *cdx4*$^{-/-}$/*sall4*^{mo} embryos could be caused by an earlier defect in LPM differentiation. The TF Scl and its cofactor Lmo2 are key determinants of hematopoietic precursors that are expressed as bilateral stripes in the LPM at the 3-somite stage (Liao et al., 1998; Thompson et al., 1998). Loss of *scl* or *lmo2* in the zebrafish leads to a lack of RBCs (Dooley et al., 2005; Patterson et al., 2005, 2007). At the 10-somite stage, *cdx4*$^{-/-}$ embryos displayed only a few posterior *scl*+ and *lmo2*+ cells, whereas *cdx4*$^{-/-}$/*sall4*^{mo} embryos showed no detectable *scl* or *lmo2* expression (Figure 4A). This suggests that early hematopoietic progenitors do not form properly in *cdx4*$^{-/-}$/*sall4*^{mo} embryos. In contrast, *cdx4*^{mo}/*sall4*^{mo} embryos have *fli1a*+ and *draculin*+ cells in the LPM, indicating that the general lateral mesoderm is present in these embryos. *myoD* (somite), *pax2a* (kidney), and *tbx16* (presomitic mesoderm) expression is minimally affected, showing that *cdx4* and

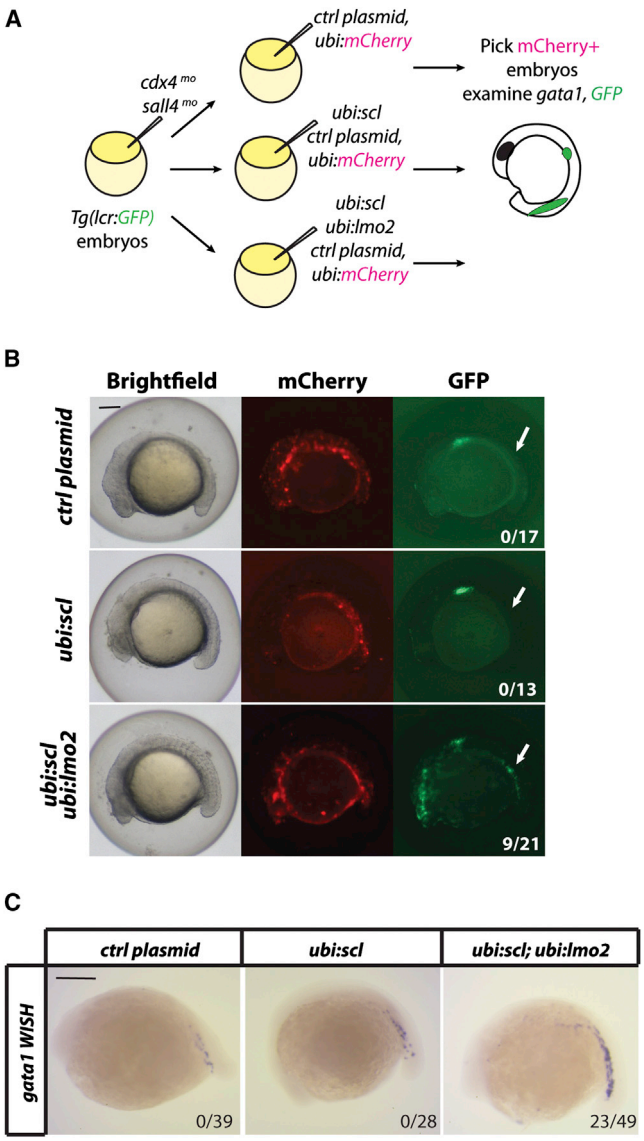

Figure 5. Overexpression of *scl* and *lmo2* Rescues the Loss of RBCs in the *cdx4*^{mo}/*sall4*^{mo} Embryos

(A) DNA-mediated overexpression scheme using Tg(*lcr:GFP*) embryos that express GFP in *globin*+ RBCs. When the embryos reached the 18-somite stage, mCherry+ embryos were selected and their GFP expression and *gata1* expression were examined.

(B) *cdx4*^{mo}/*sall4*^{mo}/*Tg(lcr:GFP)* embryos that were control plasmid injected (top), *ubi:scl* injected (middle), or *ubi:scl; ubi:lmo2* injected (bottom). The mCherry+ cells show the mosaicism. Note the GFP+ cells in the ICM (white arrow) in the bottom row. The numbers indicate the number of embryos with GFP signal in the ICM.

(C) *gata1* WISH of embryos shown in (B). The numbers indicate the number of embryos with *gata1* signal in the ICM.

All scale bars, 200 μm. See also Figure S5.

sall4 specifically affect early hematopoietic progenitors (Figure 4B; Kimmel et al., 1989; Majumdar et al., 2000; Weinberg et al., 1996). In accordance with a putative regulatory role in *scl* and *lmo2* transcription, both the Cdx4 and Sall4 ChIP-seq profiles showed both factors binding near the *scl* and *lmo2* loci, which was confirmed by ChIP-PCR analysis (Figures 5C, 5D, and S4).

To determine whether this early block in *scl* and *lmo2* expression is responsible for the RBC loss in *cdx4*$^{-/-}$/*sall4*^{mo} embryos, we overexpressed *scl* and *lmo2* in transgenic zebrafish carrying the globin *lcr:GFP* reporter (Ganis et al., 2012; Figure 5A). The *scl* and *lmo2* genes, together with a control plasmid, were driven under the control of the *ubi* promoter (Mosimann et al., 2011) and injected into *cdx4*^{mo}/*sall4*^{mo}/*Tg*(*lcr:GFP*) embryos. The *ubi:mCherry* plasmid was used as an additional control to assess injection mosaicism. As expected, injection of these plasmids led to ubiquitous expression of transgenes (Figure S5). In line with our previous results, *cdx4*^{mo}/*sall4*^{mo}/*Tg*(*lcr:GFP*) embryos lacked *lcr:GFP* expression, which could not be rescued with control plasmid injection or *ubi:scl* injection (Figure 5B, top and middle rows). In contrast, *ubi:scl; ubi:lmo2* double injection in *cdx4*^{mo}/*sall4*^{mo} embryos led to *lcr:GFP* expression in the ICM (n = 9/21; Figure 5B, bottom row), as well as *gata1* expression (n = 23/49; Figure 5C), indicating that *scl* and *lmo2* can rescue the erythropoietic defects caused by Cdx4 and Sall4 deficiency. Taken together, these results reveal that *cdx4* and *sall4* genetically interact in a regulatory circuit involving cross- and autoregulation to control the expression of TFs involved in mesodermal and hematopoietic lineage specification.

DISCUSSION

Our findings illustrate a transcriptional circuit involving Cdx4 and Sall4 that is required for the developmental transition from mesoderm to blood formation in zebrafish. By integrating ChIP-seq and expression profiling data from zebrafish embryos, we show that Sall4 shares multiple common target genes with Cdx4, including the TFs themselves, *hox* genes, *scl*, and *lmo2*. Consistent with this finding, the *cdx4*$^{-/-}$/*sall4*^{mo} embryos exhibit enhanced defects in embryonic hematopoiesis compared with *cdx4*$^{-/-}$ embryos, which can be overcome by *scl* and *lmo2* overexpression.

sall4 deficiency alone does not affect embryonic erythropoiesis, but it cooperates with the *cdx4* mutant phenotype as shown by microarray, loss of RBCs, and severe tail truncation (Figures 2, 3, S2A, and S3). Similarly, the *cdx1a*^{mo} has a mild phenotype, but *cdx4*$^{-/-}$/*cdx1a*^{mo} embryos show a more severe axial truncation and a complete loss of erythropoiesis compared with *cdx4*$^{-/-}$ (Davidson and Zon, 2006). This finding is attributed to redundancy between

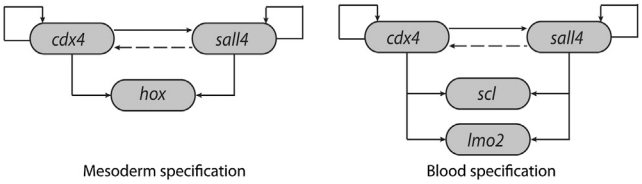

Figure 6. Model

Cdx4 and Sall4 autoregulate and cross-regulate each other (Sall4-to-Cdx4 regulation is dotted because it is unclear whether Sall4 regulates Cdx4 transcription). They regulate the LPM-to-blood transition in two ways: (1) they regulate *hox* genes for mesoderm specification, and (2) they regulate *scl* and *lmo2* for blood specification.

Cdx1a and Cdx4, given that Cdx paralogs compensate for each other (Savory et al., 2009b). Sall4 shares activities with the Cdx factors, and Sall4 binding likely enhances the transcriptional activity of Cdx-containing complexes on cobound target genes (Figure 2). Sall4 activates target genes synergistically with other TFs, such as Tcf4 and beta-catenin in gastrula-stage mouse embryos, and with Tbx5 in the heart and forelimb field (Koshiba-Takeuchi et al., 2006; Uez et al., 2008). In addition, Sall4 physically binds with Cdx2 in murine ESCs (Nishiyama et al., 2009), potentially supporting a model whereby Cdx factors and Sall4, each bound to their respective DNA consensus motifs on common targets, are able to form an enhanceosome (Nishiyama et al., 2009). Our ChIP-seq data demonstrate cobinding on DNA, suggesting that this interaction regulates the transition from mesoderm to the blood lineage.

The transcriptional program in the mesoderm adapts to the progressive development of the final descendant organs. During zebrafish development, *cdx4* is highly expressed in the future mesodermal progenitor cells during the early gastrula stage, and its expression overlaps with that of hematopoietic genes at the 3-somite stage. By the 5-somite stage, *cdx4* is expressed in the paraxial mesoderm, diverging from that of hematopoietic genes. Our ChIP-seq result suggests that during the gastrula stage, a Cdx4-Sall4 circuit regulates genes (e.g., *hox* genes) that drive cells to adopt a posterior mesodermal fate, which by the late gastrula stage allows Cdx4 to drive the expression of hematopoietic genes (Figure 2). Although the mild decrease in the expression of nonhematopoietic genes such as *pax2a* and *tbx16* in $cdx4^{mo}/sall4^{mo}$ embryos raises the question as to whether *cdx4* and *sall4* specifically affect hematopoietic tissues, these embryos still have a normal amount of *fli1a*+ *draculin*+ cells, indicating that the LPM formation is normal (Figure 4).

Scl and *Lmo2* are key hematopoietic TFs whose deficiency cause severe anemia (Dooley et al., 2005; Patterson et al., 2005; Shivdasani et al., 1995; Warren et al., 1994). As *scl* overexpression could not rescue the *gata1* loss seen in $cdx4^{-/-}$, it has been hypothesized that Cdx4 acts to make the posterior mesoderm competent to respond to genes that specify the hematopoietic fate (Davidson et al., 2003). An alternative model would include the possibility that other Cdx4 target genes participate in hematopoietic induction. One intriguing possibility is that Scl is insufficient to rescue the $cdx4^{-/-}$ because it lacks the Scl cofactor, Lmo2. Our ChIP-seq and ChIP-PCR data demonstrate that *scl* and *lmo2* genes are bound by Cdx4 and Sall4, and expression of *scl* and *lmo2* is reduced in $cdx4^{-/-}/sall4^{mo}$ (Figures 4A, 4C, 4D, and S4). Our rescue data show that *scl* in combination with *lmo2* can drive erythropoiesis genes in the $cdx4^{mo}/sall4^{mo}$, indicating that *lmo2* is another key factor that is responsible for the loss of RBCs (Figure 5). The lack of *gata1* rescue to the wild-type level shows that there could be other additional Cdx4 and Sall4 targets. A recent ChIP study showed that *Lmo2* transcription in hematopoietic cells is regulated by HoxA9 (Huang et al., 2012). Our results suggest that Cdx4 and Sall4 regulate *hoxa9a* transcription in zebrafish (Figure S2B). This suggests that *lmo2* could be regulated in a tightly controlled manner during the differentiation of LPM to blood, directly by Cdx4 and Sall4, and secondarily by another Cdx4 and Sall4 target gene, Hoxa9a. We speculate that this type of transcriptional loop ensures a robust activation of the blood program.

Our ChIP-seq data indicate that Cdx4 and Sall4 engage in auto- and cross-regulatory loops. Such regulatory circuits are frequently seen during embryonic development. For example, during segmentation of rhombomere 4 in the mouse hindbrain, retinoic acid signaling first turns on *HoxB1*, followed by *HoxB1*, *HoxB2*, and *HoxA2*, maintaining their expression through tight auto- and cross-regulatory loops (Agarwal et al., 2011; Gavalas et al., 2003; Tümpel et al., 2007). The Cdx4-Sall4 circuit during zebrafish development may function in an analogous way with upstream regulators such as Wnt, BMP, and FGF, activating expression of Cdx4 and Sall4, followed by the stabilization of their expression by auto- and cross-regulatory loops. We hypothesize that a stable Cdx4-Sall4 circuit is required to make the mesoderm competent for the specification of posterior tissue lineages such as blood by turning on the hematopoietic master TFs Scl and Lmo2 (Figure 6).

Our current model also gives insights into leukemogenesis. Previously, Hox gene misregulation was the main focus of attempts to understand the mechanism behind Cdx genes causing leukemia (Bansal et al., 2006; Scholl et al., 2007). Our current model suggests another possibility, i.e., that Cdx genes directly regulate Scl and Lmo2. As mutation of both of these genes has been linked to various leukemias, such as T cell acute lymphoblastic leukemia (Bash et al., 1995; Boehm et al., 1991; Royer-Pokora et al.,

1991), the model raises the possibility that these two genes may be aberrantly regulated in leukemias that are caused by Cdx or Sall4 mutation.

In conclusion, our data establish a Cdx4-Sall4 circuit that acts in the posterior mesoderm to facilitate blood cell formation and axial elongation. We propose that during the early gastrula stage, Cdx4 and Sall4 are activated by upstream regulators such as Wnt, and their auto- and cross-regulation act to stabilize the mesoderm state. At the end of gastrulation, Cdx4 and Sall4 bind to *scl* and *lmo2* to induce the hematopoietic program in the mesoderm. As upstream signaling dissipates, the Cdx4-Sall4 regulatory loops are disrupted, with a concomitant reduction in *cdx4* and *sall4* expression, and further blood differentiation is driven by factors such as Scl and Lmo2 (Figure 6). This model is likely applicable to the formation of other tissues and provides a molecular framework to understand how Cdx and Sall factors induce leukemia.

EXPERIMENTAL PROCEDURES

Zebrafish

Zebrafish were maintained according to Institutional Animal Care and Use Committee guidelines. The Animal Care and Use Committee of Boston Children's Hospital approved all of the animal protocols. Wild-type (Tu) and $cdx4^{+/-}$ incrossed embryos were collected at the one-cell stage and injected with mRNA or morpholino for further experiments.

ChIP

ChIP was performed as previously described (Lee et al., 2006; Lindeman et al., 2009). For detailed information, see the Supplemental Experimental Procedures. myc (abcam ab9132), H3K4me3 (Millipore 07-473), and H3K27ac (abcam ab4729) antibodies were used at 5 μg per ChIP sample.

ChIP-Seq Analysis

Sequence reads were aligned to the genome (danRer6) using Bowtie version 0.12.7 with options "-q–best–strata -m 1 -p 4–chunkmbs 1024" (Langmead et al., 2009). Only uniquely mapping reads were analyzed further. Binding events were detected using GPS as previously described (Guo et al., 2010). For detailed information on ChIP-seq analysis, see the Supplemental Experimental Procedures. The ChIP-seq data have been deposited in the GEO database under accession number GSE48254.

ChIP-PCR Analysis

Primers were designed for *cdx4*, *sall4*, *scl*, and *lmo2* loci (listed in Table S1). Quantities are expressed as fold change compared with input controls.

Morpholinos

One-cell-stage embryos were injected with $sall4^{mo}$ (2 ng; Harvey and Logan, 2006), $cdx4^{mo}$ (1.5 ng), or $cdx1a^{mo}$ (0.5 ng).

mRNA

cdx4 and *sall4* cDNA was described previously (Davidson et al., 2003; Harvey and Logan, 2006). mRNA was generated by the mMessage mMachine kit and injected into one-cell-stage embryos.

Microarray Analysis

Embryos were injected with either *cdx4* or *sall4*, or both morpholinos together. Injected embryos, along with uninjected control embryos, were harvested at the 3- or 10-somite stage and RNA was prepared for microarray. For the arrays in these experiments, we used the prerelease Affymetrix Zebrafish 2.0 array, which was developed in the Zon laboratory in cooperation with Affymetrix. The $cdx4^{mo}/cdx1a^{mo}$ data set was generated on the Affymetrix Zebrafish 1.0 array. Detailed information on microarray analysis can be found in the Supplemental Experimental Procedures.

GSEA Analysis

Enrichment of Cdx4-Bound Genes in the cdx4/cdx1a Double-Morphant Gene-Expression Set

The fli1a:GFP or scl^{mo} gene lists were used as input to GSEA for queries into the entire $cdx4^{mo}/sall4^{mo}$ microarray data set. In this case, because the $cdx4^{mo}/sall4^{mo}$ arrays were performed using the Zebrafish Affymetrix 2.0 arrays, we used the Zv9 gene identifier as the input for GSEA. For endothelial, kidney, muscle, and neuron gene sets, the annotated gene list was probed. Enrichment of the double morphant compared with control embryos was calculated using the NES and FDR as described above. Detailed information regarding the gene list sources can be found in the Supplemental Experimental Procedures.

WISH and o-Dianisidine Staining

WISH and o-dianisidine staining were performed as previously described (Ransom et al., 1996; Thisse et al., 1993). The *gata1*, *sall4*, *scl*, *lmo2*, *fli1a*, *myoD*, *draculin*, *pax2a*, *tbx16*, and *morc3b* probes were described in previous publications (Detrich et al., 1995; Kimmel et al., 1989; Liao et al., 1998; Majumdar et al., 2000; Thompson et al., 1998; Weinberg et al., 1996).

DNA Injection

For DNA injection, 1 nl of a 16 ng/μl DNA mixture was injected into one-cell-stage embryos. For detailed information on the plasmids used, see the Supplemental Experimental Procedures and Table S2.

SUPPLEMENTAL INFORMATION

Supplemental Information includes Supplemental Experimental Procedures, five figures, and two tables and can be found with this article online at http://dx.doi.org/10.1016/j.stemcr.2013.10.001.

ACKNOWLEDGMENTS

We thank members of the Zon laboratory for helpful discussions, J. Ganis for providing *Tg(lcr:GFP)*, and M. Logan for providing the *sall4* cDNA construct. We also thank the Whitehead Genome Technology Core for data production and analysis support. Microarray

studies were performed by the Molecular Genetics Core Facility at Children's Hospital Boston, supported by NIH grants P50-NS40828 and P30-HD18655. This work was supported by grants from the NHLBI (5R01HL048801-21 to L.I.Z. and 5P01HL32262-31), NIDDK (5P30 DK49126-19, DK53298-15, and R24 DK092760-02), and HHMI (to L.I.Z.). L.I.Z. is a founder and stockholder of Fate, Inc., and Scholar Rock, and a scientific advisor for Stemgent.

Received: February 26, 2013
Revised: October 1, 2013
Accepted: October 2, 2013
Published: November 7, 2013

REFERENCES

Agarwal, P., Verzi, M.P., Nguyen, T., Hu, J., Ehlers, M.L., McCulley, D.J., Xu, S.M., Dodou, E., Anderson, J.P., Wei, M.L., and Black, B.L. (2011). The MADS box transcription factor MEF2C regulates melanocyte development and is a direct transcriptional target and partner of SOX10. Development *138*, 2555–2565.

Bailey, T.L., and Elkan, C. (1994). Fitting a mixture model by expectation maximization to discover motifs in biopolymers. Proc. Int. Conf. Intell. Syst. Mol. Biol. *2*, 28–36.

Bansal, D., Scholl, C., Fröhling, S., McDowell, E., Lee, B.H., Döhner, K., Ernst, P., Davidson, A.J., Daley, G.Q., Zon, L.I., et al. (2006). Cdx4 dysregulates Hox gene expression and generates acute myeloid leukemia alone and in cooperation with Meis1a in a murine model. Proc. Natl. Acad. Sci. USA *103*, 16924–16929.

Barembaum, M., and Bronner-Fraser, M. (2004). A novel spalt gene expressed in branchial arches affects the ability of cranial neural crest cells to populate sensory ganglia. Neuron Glia Biol. *1*, 57–63.

Bash, R.O., Hall, S., Timmons, C.F., Crist, W.M., Amylon, M., Smith, R.G., and Baer, R. (1995). Does activation of the TAL1 gene occur in a majority of patients with T-cell acute lymphoblastic leukemia? A pediatric oncology group study. Blood *86*, 666–676.

Boehm, T., Foroni, L., Kaneko, Y., Perutz, M.F., and Rabbitts, T.H. (1991). The rhombotin family of cysteine-rich LIM-domain oncogenes: distinct members are involved in T-cell translocations to human chromosomes 11p15 and 11p13. Proc. Natl. Acad. Sci. USA *88*, 4367–4371.

Charité, J., de Graaff, W., Consten, D., Reijnen, M.J., Korving, J., and Deschamps, J. (1998). Transducing positional information to the Hox genes: critical interaction of cdx gene products with position-sensitive regulatory elements. Development *125*, 4349–4358.

Chawengsaksophak, K., de Graaff, W., Rossant, J., Deschamps, J., and Beck, F. (2004). Cdx2 is essential for axial elongation in mouse development. Proc. Natl. Acad. Sci. USA *101*, 7641–7645.

Davidson, A.J., Ernst, P., Wang, Y., Dekens, M.P., Kingsley, P.D., Palis, J., Korsmeyer, S.J., Daley, G.Q., and Zon, L.I. (2003). cdx4 mutants fail to specify blood progenitors and can be rescued by multiple hox genes. Nature *425*, 300–306.

Davidson, A.J., and Zon, L.I. (2004). The 'definitive' (and 'primitive') guide to zebrafish hematopoiesis. Oncogene *23*, 7233–7246.

Davidson, A.J., and Zon, L.I. (2006). The caudal-related homeobox genes cdx1a and cdx4 act redundantly to regulate hox gene expression and the formation of putative hematopoietic stem cells during zebrafish embryogenesis. Dev. Biol. *292*, 506–518.

de la Serna, I.L., Ohkawa, Y., Berkes, C.A., Bergstrom, D.A., Dacwag, C.S., Tapscott, S.J., and Imbalzano, A.N. (2005). MyoD targets chromatin remodeling complexes to the myogenin locus prior to forming a stable DNA-bound complex. Mol. Cell. Biol. *25*, 3997–4009.

Detrich, H.W., 3rd, Kieran, M.W., Chan, F.Y., Barone, L.M., Yee, K., Rundstadler, J.A., Pratt, S., Ransom, D., and Zon, L.I. (1995). Intraembryonic hematopoietic cell migration during vertebrate development. Proc. Natl. Acad. Sci. USA *92*, 10713–10717.

Dooley, K.A., Davidson, A.J., and Zon, L.I. (2005). Zebrafish scl functions independently in hematopoietic and endothelial development. Dev. Biol. *277*, 522–536.

Frei, E., Schuh, R., Baumgartner, S., Burri, M., Noll, M., Jürgens, G., Seifert, E., Nauber, U., and Jäckle, H. (1988). Molecular characterization of spalt, a homeotic gene required for head and tail development in the Drosophila embryo. EMBO J. *7*, 197–204.

Galloway, J.L., Wingert, R.A., Thisse, C., Thisse, B., and Zon, L.I. (2008). Combinatorial regulation of novel erythroid gene expression in zebrafish. Exp. Hematol. *36*, 424–432.

Ganis, J.J., Hsia, N., Trompouki, E., de Jong, J.L., DiBiase, A., Lambert, J.S., Jia, Z., Sabo, P.J., Weaver, M., Sandstrom, R., et al. (2012). Zebrafish globin switching occurs in two developmental stages and is controlled by the LCR. Dev. Biol. *366*, 185–194.

Gao, N., White, P., and Kaestner, K.H. (2009). Establishment of intestinal identity and epithelial-mesenchymal signaling by Cdx2. Dev. Cell *16*, 588–599.

Gavalas, A., Ruhrberg, C., Livet, J., Henderson, C.E., and Krumlauf, R. (2003). Neuronal defects in the hindbrain of Hoxa1, Hoxb1 and Hoxb2 mutants reflect regulatory interactions among these Hox genes. Development *130*, 5663–5679.

Guo, Y., Papachristoudis, G., Altshuler, R.C., Gerber, G.K., Jaakkola, T.S., Gifford, D.K., and Mahony, S. (2010). Discovering homotypic binding events at high spatial resolution. Bioinformatics *26*, 3028–3034.

Harvey, S.A., and Logan, M.P. (2006). sall4 acts downstream of tbx5 and is required for pectoral fin outgrowth. Development *133*, 1165–1173.

Huang, Y., Sitwala, K., Bronstein, J., Sanders, D., Dandekar, M., Collins, C., Robertson, G., MacDonald, J., Cezard, T., Bilenky, M., et al. (2012). Identification and characterization of Hoxa9 binding sites in hematopoietic cells. Blood *119*, 388–398.

Jürgens, G. (1988). Head and tail development of the Drosophila embryo involves spalt, a novel homeotic gene. EMBO J. *7*, 189–196.

Kimmel, C.B., Kane, D.A., Walker, C., Warga, R.M., and Rothman, M.B. (1989). A mutation that changes cell movement and cell fate in the zebrafish embryo. Nature *337*, 358–362.

Knittel, T., Kessel, M., Kim, M.H., and Gruss, P. (1995). A conserved enhancer of the human and murine Hoxa-7 gene specifies the anterior boundary of expression during embryonal development. Development *121*, 1077–1088.

Koshiba-Takeuchi, K., Takeuchi, J.K., Arruda, E.P., Kathiriya, I.S., Mo, R., Hui, C.C., Srivastava, D., and Bruneau, B.G. (2006).

Cooperative and antagonistic interactions between Sall4 and Tbx5 pattern the mouse limb and heart. Nat. Genet. *38*, 175–183.

Langmead, B., Trapnell, C., Pop, M., and Salzberg, S.L. (2009). Ultrafast and memory-efficient alignment of short DNA sequences to the human genome. Genome Biol. *10*, R25.

Lawson, N.D., and Weinstein, B.M. (2002). In vivo imaging of embryonic vascular development using transgenic zebrafish. Dev. Biol. *248*, 307–318.

Lee, T.I., Johnstone, S.E., and Young, R.A. (2006). Chromatin immunoprecipitation and microarray-based analysis of protein location. Nat. Protoc. *1*, 729–748.

Lein, E.S., Hawrylycz, M.J., Ao, N., Ayres, M., Bensinger, A., Bernard, A., Boe, A.F., Boguski, M.S., Brockway, K.S., Byrnes, E.J., et al. (2007). Genome-wide atlas of gene expression in the adult mouse brain. Nature *445*, 168–176.

Liao, E.C., Paw, B.H., Oates, A.C., Pratt, S.J., Postlethwait, J.H., and Zon, L.I. (1998). SCL/Tal-1 transcription factor acts downstream of cloche to specify hematopoietic and vascular progenitors in zebrafish. Genes Dev. *12*, 621–626.

Lim, C.Y., Tam, W.L., Zhang, J., Ang, H.S., Jia, H., Lipovich, L., Ng, H.H., Wei, C.L., Sung, W.K., Robson, P., et al. (2008). Sall4 regulates distinct transcription circuitries in different blastocyst-derived stem cell lineages. Cell Stem Cell *3*, 543–554.

Lindeman, L.C., Vogt-Kielland, L.T., Aleström, P., and Collas, P. (2009). Fish'n ChIPs: chromatin immunoprecipitation in the zebrafish embryo. Methods Mol. Biol. *567*, 75–86.

Loh, Y.H., Wu, Q., Chew, J.L., Vega, V.B., Zhang, W., Chen, X., Bourque, G., George, J., Leong, B., Liu, J., et al. (2006). The Oct4 and Nanog transcription network regulates pluripotency in mouse embryonic stem cells. Nat. Genet. *38*, 431–440.

Ma, Y., Cui, W., Yang, J., Qu, J., Di, C., Amin, H.M., Lai, R., Ritz, J., Krause, D.S., and Chai, L. (2006). SALL4, a novel oncogene, is constitutively expressed in human acute myeloid leukemia (AML) and induces AML in transgenic mice. Blood *108*, 2726–2735.

Majumdar, A., Lun, K., Brand, M., and Drummond, I.A. (2000). Zebrafish no isthmus reveals a role for pax2.1 in tubule differentiation and patterning events in the pronephric primordia. Development *127*, 2089–2098.

Morley, R.H., Lachani, K., Keefe, D., Gilchrist, M.J., Flicek, P., Smith, J.C., and Wardle, F.C. (2009). A gene regulatory network directed by zebrafish No tail accounts for its roles in mesoderm formation. Proc. Natl. Acad. Sci. USA *106*, 3829–3834.

Mosimann, C., Kaufman, C.K., Li, P., Pugach, E.K., Tamplin, O.J., and Zon, L.I. (2011). Ubiquitous transgene expression and Cre-based recombination driven by the ubiquitin promoter in zebrafish. Development *138*, 169–177.

Neff, A.W., King, M.W., Harty, M.W., Nguyen, T., Calley, J., Smith, R.C., and Mescher, A.L. (2005). Expression of Xenopus XlSALL4 during limb development and regeneration. Dev. Dyn. *233*, 356–367.

Nishiyama, A., Xin, L., Sharov, A.A., Thomas, M., Mowrer, G., Meyers, E., Piao, Y., Mehta, S., Yee, S., Nakatake, Y., et al. (2009). Uncovering early response of gene regulatory networks in ESCs by systematic induction of transcription factors. Cell Stem Cell *5*, 420–433.

O'Brien, L.L., Grimaldi, M., Kostun, Z., Wingert, R.A., Selleck, R., and Davidson, A.J. (2011). Wt1a, Foxc1a, and the Notch mediator Rbpj physically interact and regulate the formation of podocytes in zebrafish. Dev. Biol. *358*, 318–330.

Orkin, S.H., and Zon, L.I. (2008). Hematopoiesis: an evolving paradigm for stem cell biology. Cell *132*, 631–644.

Patterson, L.J., Gering, M., and Patient, R. (2005). Scl is required for dorsal aorta as well as blood formation in zebrafish embryos. Blood *105*, 3502–3511.

Patterson, L.J., Gering, M., Eckfeldt, C.E., Green, A.R., Verfaillie, C.M., Ekker, S.C., and Patient, R. (2007). The transcription factors Scl and Lmo2 act together during development of the hemangioblast in zebrafish. Blood *109*, 2389–2398.

Pownall, M.E., Tucker, A.S., Slack, J.M., and Isaacs, H.V. (1996). eFGF, Xcad3 and Hox genes form a molecular pathway that establishes the anteroposterior axis in Xenopus. Development *122*, 3881–3892.

Rada-Iglesias, A., Bajpai, R., Swigut, T., Brugmann, S.A., Flynn, R.A., and Wysocka, J. (2011). A unique chromatin signature uncovers early developmental enhancers in humans. Nature *470*, 279–283.

Ransom, D.G., Haffter, P., Odenthal, J., Brownlie, A., Vogelsang, E., Kelsh, R.N., Brand, M., van Eeden, F.J., Furutani-Seiki, M., Granato, M., et al. (1996). Characterization of zebrafish mutants with defects in embryonic hematopoiesis. Development *123*, 311–319.

Rao, S., Zhen, S., Roumiantsev, S., McDonald, L.T., Yuan, G.C., and Orkin, S.H. (2010). Differential roles of Sall4 isoforms in embryonic stem cell pluripotency. Mol. Cell. Biol. *30*, 5364–5380.

Royer-Pokora, B., Loos, U., and Ludwig, W.D. (1991). TTG-2, a new gene encoding a cysteine-rich protein with the LIM motif, is overexpressed in acute T-cell leukaemia with the t(11;14)(p13;q11). Oncogene *6*, 1887–1893.

Sandmann, T., Jensen, L.J., Jakobsen, J.S., Karzynski, M.M., Eichenlaub, M.P., Bork, P., and Furlong, E.E. (2006). A temporal map of transcription factor activity: mef2 directly regulates target genes at all stages of muscle development. Dev. Cell *10*, 797–807.

Sandmann, T., Girardot, C., Brehme, M., Tongprasit, W., Stolc, V., and Furlong, E.E. (2007). A core transcriptional network for early mesoderm development in Drosophila melanogaster. Genes Dev. *21*, 436–449.

Savory, J.G., Bouchard, N., Pierre, V., Rijli, F.M., De Repentigny, Y., Kothary, R., and Lohnes, D. (2009a). Cdx2 regulation of posterior development through non-Hox targets. Development *136*, 4099–4110.

Savory, J.G., Pilon, N., Grainger, S., Sylvestre, J.R., Béland, M., Houle, M., Oh, K., and Lohnes, D. (2009b). Cdx1 and Cdx2 are functionally equivalent in vertebral patterning. Dev. Biol. *330*, 114–122.

Scholl, C., Bansal, D., Döhner, K., Eiwen, K., Huntly, B.J., Lee, B.H., Rücker, F.G., Schlenk, R.F., Bullinger, L., Döhner, H., et al. (2007). The homeobox gene CDX2 is aberrantly expressed in most cases of acute myeloid leukemia and promotes leukemogenesis. J. Clin. Invest. *117*, 1037–1048.

Shimizu, T., Bae, Y.K., and Hibi, M. (2006). Cdx-Hox code controls competence for responding to Fgfs and retinoic acid in zebrafish neural tissue. Development *133*, 4709–4719.

Shivdasani, R.A., Mayer, E.L., and Orkin, S.H. (1995). Absence of blood formation in mice lacking the T-cell leukaemia oncoprotein tal-1/SCL. Nature *373*, 432–434.

Skromne, I., Thorsen, D., Hale, M., Prince, V.E., and Ho, R.K. (2007). Repression of the hindbrain developmental program by Cdx factors is required for the specification of the vertebrate spinal cord. Development *134*, 2147–2158.

Subramanian, V., Meyer, B.I., and Gruss, P. (1995). Disruption of the murine homeobox gene Cdx1 affects axial skeletal identities by altering the mesodermal expression domains of Hox genes. Cell *83*, 641–653.

Subramanian, A., Tamayo, P., Mootha, V.K., Mukherjee, S., Ebert, B.L., Gillette, M.A., Paulovich, A., Pomeroy, S.L., Golub, T.R., Lander, E.S., and Mesirov, J.P. (2005). Gene set enrichment analysis: a knowledge-based approach for interpreting genome-wide expression profiles. Proc. Natl. Acad. Sci. USA *102*, 15545–15550.

Thisse, C., Thisse, B., Schilling, T.F., and Postlethwait, J.H. (1993). Structure of the zebrafish snail1 gene and its expression in wild-type, spadetail and no tail mutant embryos. Development *119*, 1203–1215.

Thompson, M.A., Ransom, D.G., Pratt, S.J., MacLennan, H., Kieran, M.W., Detrich, H.W., 3rd, Vail, B., Huber, T.L., Paw, B., Brownlie, A.J., et al. (1998). The cloche and spadetail genes differentially affect hematopoiesis and vasculogenesis. Dev. Biol. *197*, 248–269.

Tümpel, S., Cambronero, F., Ferretti, E., Blasi, F., Wiedemann, L.M., and Krumlauf, R. (2007). Expression of Hoxa2 in rhombomere 4 is regulated by a conserved cross-regulatory mechanism dependent upon Hoxb1. Dev. Biol. *302*, 646–660.

Uez, N., Lickert, H., Kohlhase, J., de Angelis, M.H., Kühn, R., Wurst, W., and Floss, T. (2008). Sall4 isoforms act during proximal-distal and anterior-posterior axis formation in the mouse embryo. Genesis *46*, 463–477.

van den Akker, E., Forlani, S., Chawengsaksophak, K., de Graaff, W., Beck, F., Meyer, B.I., and Deschamps, J. (2002). Cdx1 and Cdx2 have overlapping functions in anteroposterior patterning and posterior axis elongation. Development *129*, 2181–2193.

van den Berg, D.L., Snoek, T., Mullin, N.P., Yates, A., Bezstarosti, K., Demmers, J., Chambers, I., and Poot, R.A. (2010). An Oct4-centered protein interaction network in embryonic stem cells. Cell Stem Cell *6*, 369–381.

van Nes, J., de Graaff, W., Lebrin, F., Gerhard, M., Beck, F., and Deschamps, J. (2006). The Cdx4 mutation affects axial development and reveals an essential role of Cdx genes in the ontogenesis of the placental labyrinth in mice. Development *133*, 419–428.

Verzi, M.P., Shin, H., He, H.H., Sulahian, R., Meyer, C.A., Montgomery, R.K., Fleet, J.C., Brown, M., Liu, X.S., and Shivdasani, R.A. (2010). Differentiation-specific histone modifications reveal dynamic chromatin interactions and partners for the intestinal transcription factor CDX2. Dev. Cell *19*, 713–726.

Verzi, M.P., Shin, H., Ho, L.L., Liu, X.S., and Shivdasani, R.A. (2011). Essential and redundant functions of caudal family proteins in activating adult intestinal genes. Mol. Cell. Biol. *31*, 2026–2039.

Wang, Y., Yates, F., Naveiras, O., Ernst, P., and Daley, G.Q. (2005). Embryonic stem cell-derived hematopoietic stem cells. Proc. Natl. Acad. Sci. USA *102*, 19081–19086.

Wang, Y., Yabuuchi, A., McKinney-Freeman, S., Ducharme, D.M., Ray, M.K., Chawengsaksophak, K., Archer, T.K., and Daley, G.Q. (2008). Cdx gene deficiency compromises embryonic hematopoiesis in the mouse. Proc. Natl. Acad. Sci. USA *105*, 7756–7761.

Warren, A.J., Colledge, W.H., Carlton, M.B., Evans, M.J., Smith, A.J., and Rabbitts, T.H. (1994). The oncogenic cysteine-rich LIM domain protein rbtn2 is essential for erythroid development. Cell *78*, 45–57.

Wei, W., Wen, L., Huang, P., Zhang, Z., Chen, Y., Xiao, A., Huang, H., Zhu, Z., Zhang, B., and Lin, S. (2008). Gfi1.1 regulates hematopoietic lineage differentiation during zebrafish embryogenesis. Cell Res. *18*, 677–685.

Weinberg, E.S., Allende, M.L., Kelly, C.S., Abdelhamid, A., Murakami, T., Andermann, P., Doerre, O.G., Grunwald, D.J., and Riggleman, B. (1996). Developmental regulation of zebrafish MyoD in wild-type, no tail and spadetail embryos. Development *122*, 271–280.

Wingert, R.A., and Davidson, A.J. (2011). Zebrafish nephrogenesis involves dynamic spatiotemporal expression changes in renal progenitors and essential signals from retinoic acid and irx3b. Dev. Dyn. *240*, 2011–2027.

Wingert, R.A., Selleck, R., Yu, J., Song, H.D., Chen, Z., Song, A., Zhou, Y., Thisse, B., Thisse, C., McMahon, A.P., and Davidson, A.J. (2007). The cdx genes and retinoic acid control the positioning and segmentation of the zebrafish pronephros. PLoS Genet. *3*, 1922–1938.

Wong, K.S., Proulx, K., Rost, M.S., and Sumanas, S. (2009). Identification of vasculature-specific genes by microarray analysis of Etsrp/Etv2 overexpressing zebrafish embryos. Dev. Dyn. *238*, 1836–1850.

Wu, Q., Chen, X., Zhang, J., Loh, Y.H., Low, T.Y., Zhang, W., Zhang, W., Sze, S.K., Lim, B., and Ng, H.H. (2006). Sall4 interacts with Nanog and co-occupies Nanog genomic sites in embryonic stem cells. J. Biol. Chem. *281*, 24090–24094.

Xu, C., Fan, Z.P., Müller, P., Fogley, R., DiBiase, A., Trompouki, E., Unternaehrer, J., Xiong, F., Torregroza, I., Evans, T., et al. (2012). Nanog-like regulates endoderm formation through the Mxtx2-Nodal pathway. Dev. Cell *22*, 625–638.

Young, T., and Deschamps, J. (2009). Hox, Cdx, and anteroposterior patterning in the mouse embryo. Curr. Top. Dev. Biol. *88*, 235–255.

Young, T., Rowland, J.E., van de Ven, C., Bialecka, M., Novoa, A., Carapuco, M., van Nes, J., de Graaff, W., Duluc, I., Freund, J.N., et al. (2009). Cdx and Hox genes differentially regulate posterior axial growth in mammalian embryos. Dev. Cell *17*, 516–526.